Edge-Membership Based Blurred Image Reconstruction Algorithm

Wei-De Chang [*], Jian-Jiun Ding [*], Yu Chen [*], Chir-Weei Chang [†], and Chuan-Chung Chang [†]
[*] Department of Electrical Engineering, National Taiwan University, Taiwan, R.O.C.
Email: r99942113@ee.ntu.edu.tw, djj@cc.ee.ntu.edu.tw, hck13kimo@gmail.com, TEL: +886-2-33669652
[†] Electronics and Optoelectronics Research Laboratories, Industrial Technology Research Institute, Hsinchu, Taiwan, R.O.C.
Email: ChirWeeiChang@itri.org.tw, ChuanChungChang@itri.org.tw, TEL: +886-3-5918384

***Abstract*— Enhancing the sharpness of edges and avoiding the ringing effect are two important issues in blurred image reconstruction. However, there is a tradeoff between the two goals. A reconstruction filter with long impulse response can reduce the ringing artifact, however, the sharpness of the edge is decreased. By contrast, a short impulse response reconstruction filter can perfectly retrieve the edge but is not robust to noise. In this paper, an edge-membership based blurred image reconstruction algorithm is proposed. In order to achieve the two goals simultaneously, we design two filters. One focuses on edge restoration and the other one focuses on noise removing. After performing linear combination of the outputs of the two reconstruction filters, the edges are preserved and the ringing artifacts are removed at the same time. Simulation results show that our approach can reconstruct the blurred image with sharp edge and less ringing effect.**

I. INTRODUCTION

A blurred image B can be modeled by the following equation:

$$B = I \otimes K + M \tag{1}$$

where I is the original image, K is the point spread function (PSF) [1], M is noise, and $\otimes$ is the convolution operator. The goal of image deblurring is to reconstruct a true image from the defocused image B.

Image deblurring can be categorized into two types: blind deconvolution and non-blind deconvolution. If the PSF is unknown, the problem is called blind deconvolution; furthermore, if the PSF is known, the problem is called non-blind deconvolution. A comprehensive literature review can be found in [2].

Referring to [3], non-blind deconvolution has been used for many classical methods, such as the Wiener filter [3] [4], the Kalman filter [5], and Tikhonov regularization. Moreover, the edge-preserving regularization [6] is proposed to restore the blurred image with strong regularization for smooth regions and weak regularization for the sharp edge, and it can be used in non-Gaussian prior, such as the RL algorithm [7].

However, even with a known kernel, non-blind deconvolution is still under-constrained. The ringing artifacts are inevitable because the kernel is often band-limited with a sharp frequency cut off, and there will be zero values or near-zero values in its frequency response. At those frequencies, the direct inverse of the kernel usually has a very large magnitude, and it will cause the amplifying signal and noise rate. Moreover, the noise due to the sensor also amplifies the ringing artifacts.

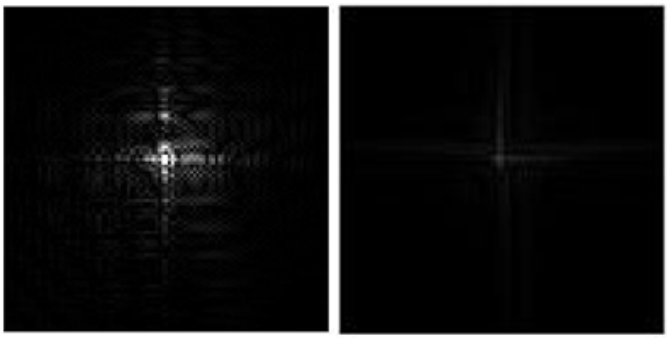

(a) (b)

Fig. 1 (a) The reconstruction filter for flat regions. (b) The reconstruction filter for edge.

On the other hand, if the reconstruction filter is designed for reconstructing the sharp edge, the retrieved image will have better performance in the edge region. However, the ringing artifacts are produced at the flat region, as shown in Fig. 1(a). Moreover, if the reconstruction filter focuses on flat regions, the restored image is robust to noise but with poor performance in edge. See Fig. 1(b).

In this paper, we utilize the Wiener filter as our core technique which is classified as the non-blind deconvolution. In our algorithm, we first establish two reconstruction filters. One is designed for restoring flat region and another is focus on processing the edge reconstruction. According to the gradient map, the edge parts of restored image are allocated to the result of applying narrow filter and the flat regions of restored image are allocated to the result of applying wide filter. After assembling those two parts, the restored image is finally obtained with the sharp edge and few ringing.

This paper is organized as follows. In Section II, we briefly revisit the Wiener filter which is a core technique in our algorithm. In Section III, we introduce our edge-membership based reconstruction filter; moreover, the kernel calculation methods are illustrated in this section. In Section IV, the simulation results is presented, we also show the comparison table of MSE and SSIM [8] in end of this section. A conclusion is made in Section V.

II. WIENER FILTER DESIGN IN THE FREQUENCY DOMAIN

In our algorithm, the Wiener filter for image reconstruction is employed to restore an optical blurred model, and there are many forms of mathematical expressions. In this section, the

Wiener filter will be revisited to have a new cost function, and the filter coefficients is obtain in the end of this section.

Let $I(F)$ and $B(F)$ be the reference image and the blurred image of the blurred model in the frequency domain, the blurred image is expressed as follows:

$$B(F) = I(F)K(F) + M(F) \tag{2}$$

where $K(F)$ is the Fourier transform (FT) of the PSF and $M(F)$ is the FT of the additive noise. The restored image $\hat{I}(F)$ can be reconstructed by a filter $H(F)$ as follows:

$$\hat{I}(F) = B(F)H(F). \tag{3}$$

In order to find out the coefficients of $H(F)$, which can be solved by taking the partial derivative of the energy of the error function $E_r(F)$ to be

$$E\left(\frac{\partial\int|E_r(F)|^2 dF}{\partial H(F)}\right) = E\left\{-|I(F)|^2 K(F) + |I(F)|^2 |K(F)|^2 H(-F) + H(-F)|M(F)|^2\right\} \tag{4}$$

where

$$E_r(F) = I(F) - \left[I(F)K(F) + M(F)\right]H(F). \tag{5}$$

After setting (5) to zero, and $E(M(F))$ is assumed to zero, the reconstruction filter $H(F)$ can be obtained

$$H(F) = \frac{1}{\frac{E\left(|M(F)|^2\right)}{|I(F)|^2 K^*(F)} + K(F)} \tag{6}$$

where MF is an additive noise in frequency domain.

In (6), a new reconstruction filter $H(F)$ is proposed. Instead of using the Wiener reconstruction filter in [9] which has the inaccurate estimation of the blurring coefficient because the filter has no consideration of the noise, the new filter can be adaptively designed for different noise. Thus, the better performance is produced due to the adjustable filter types against to noise.

III. Proposed Edge-Membership Based Image Reconstruction Algorithm

In the image reconstruction system, the ringing artifacts are inevitable since the blurred kernel is often bandlimited with a sharp frequency cutoff, and there will be zero values or near-zero values in its frequency response. At these frequencies response, it will generate the very large amplitude by direct inverse of the blurred kernel, causing the excessive amplification of signal and noise.

Before the proposed edge-membership based image reconstruction algorithm is introduced, we first illustrate our method of the blurred kernel estimation. In our approach, in order to invent the ripple-like ringing from the direct inverse in the specific frequency which with the zero values or near-zero values, we give a non-zero value to replace it. After the process, the ringing artifacts produced by direct inverse are significantly reduced.

In the image deblurring procedure, the purpose of reconstruction filter is usually designed for the sharp edge. However, since the ringing artifacts are always produced in the smooth regions around the boundary in the deconvolution procedure, there is a tradeoff between the smooth regions and the sharp edges due to the filter designed problem. To obtain the sharp edges, the performance reduction problem of the noise amplification in the smooth regions is produced. Moreover, in order to acquire higher performance in the smooth region against to noise, the filter is designed to have flatter outlook which directly affect the edge performance.

In our approach, we reform the Wiener filter in (6). First, an assumption of our image reconstruction filter is used that the true image can be approximated as follows if $I[n]$ is the edge type image:

$$I[n] = \begin{cases} 0 & \text{, for n<0} \\ \lim_{\sigma\to 0}\exp(-\sigma n) & \text{, for n} \geq 0 \end{cases} \tag{7}$$

where σ is the adjustable parameter.

After performing the Fourier transform, the target image $I[n]$ can be written as

$$I(F) = \lim_{\sigma\to 0}\sum_{n=0}^{\infty} e^{-j2\pi Fn}e^{-\sigma\pi} \cong \frac{e^{j\pi F}}{j2\sin(\pi F)} \tag{8}$$

Suppose that the noise is stationary and white and the energy is equal to μ, i.e., $E\left(|m[n]|^2\right) = \mu$ where $E\{\cdot\}$ denotes the expectation operation. According to Parseval's theorem

$$\int_{-0.5}^{0.5} E\left(|M(F)|^2\right)dF = \sum_n E\left(|m[n]|^2\right) = \sum_n \mu \tag{9}$$

After assuming the designed filter is FIR filter and the length is N_2, we can obtain the energy of noise

$$E\left(|M(F)|^2\right) = N_2\mu \tag{10}$$

According to (8) and (10), the reconstruction filter in (6) can be obtained

$$H(F) = \frac{1}{N\frac{4\sin^2(\pi F)}{K^*(F)} + K(F)} \tag{11}$$

where N is an adjustable parameter of the energy of noise equal to $N_2\mu$ that can be control to decide the width of the reconstruction filter.

In (11), the noise-dependent reconstruction filter is designed. If the parameter N is set to be a large value, the width of the reconstruction filter outlook is broader; on the contrary, if the parameter N is set to be a small value, the width of the reconstruction outlook is narrow. The broad filter has the good performance against to noise which is suitable to restore the blurred image in the smooth regions. However, the edge sharpness of the restored image will be reduced simultaneously. On the other hand, the narrow filter has the good performance to the edge performance. However, the noise amplification problem of the restored image is produced in the smooth regions.

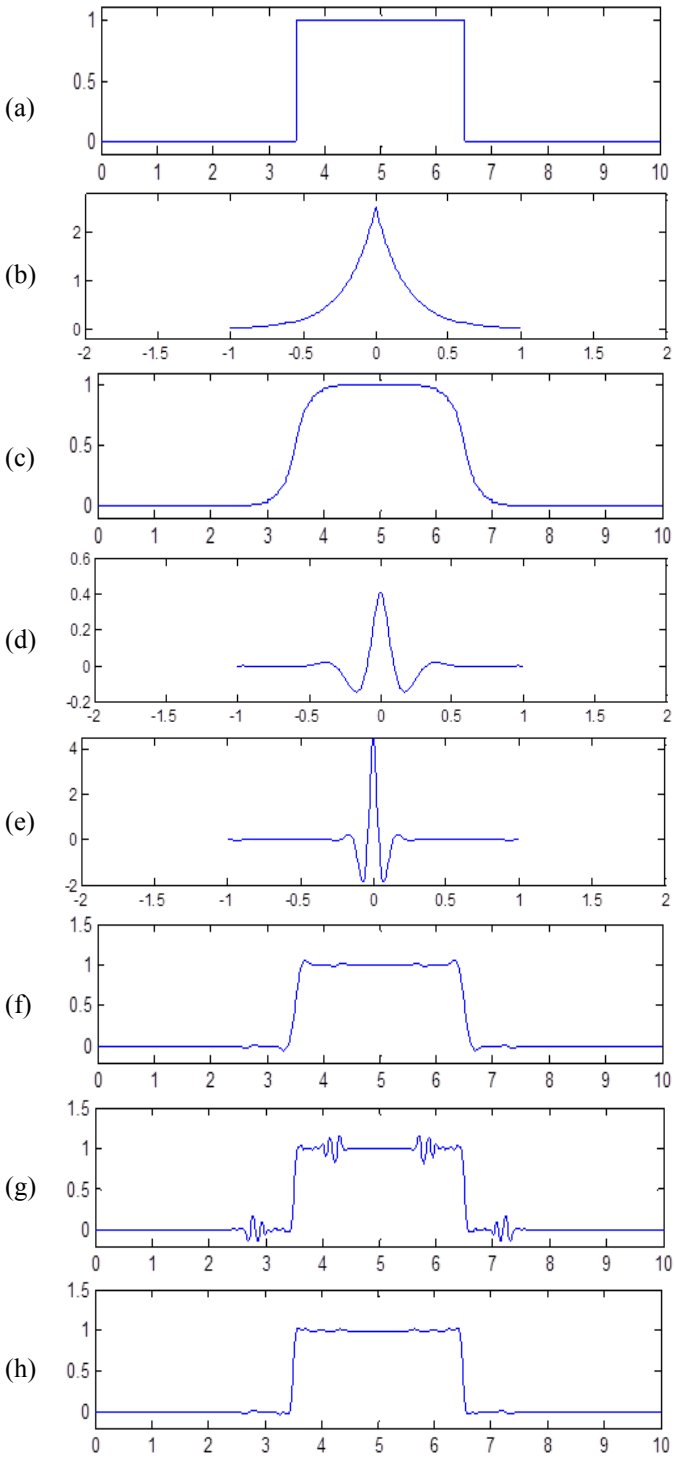

Fig. 2 (a) Target signal. (b) Point spread function (PSF). (c) Blurred signal. (d) The reconstruction filter suit for non-edge region: $u[n]$. (e) The reconstruction filter suit for edge region: $v[n]$. (f) The result of using $u[n]$ (better performance in the **flat region**). (g) The result of using $v[n]$ (better performance in the **edge region**). (h) The result of using edge-membership based reconstruction filter (better performance in **both flat and edge regions**).

To obtain the balance performance between the edge regions and the smooth regions, we proposed an edge-membership based algorithm which give different weights on two distinct parameters N in (11). The weighting function is

$$w(t) = 0.5 + 0.5\tanh\left\{w_0\left(G[n] - s_0\right)\right\} \qquad (12)$$

where $G[n]$ is a gradient map; furthermore, w_0 and s_0 are the adjustable parameter. We suggest that w_0 can be selected as a larger value and s_0 should be larger than the variation caused from noise. After the weighting function is given, the better performance of the restored image is obtained.

Fig. 2 shows 1-D simulation results of our edge-membership based reconstruction filter. Fig. 2 (a) is a target signal, and a blurred signal is infected from a point spread function in Fig. 2(b). The two reconstruction filter we designed are in Figs. 2(d) and 2(e), called $u[n]$ and $v[n]$. After restoring the blurred signal from $u[n]$ and $v[n]$, Fig. 2 (f) and (g) are obtained. The restored signal reconstructed from the broader filter has few ringing artifact, but the resulting edge is not sharp. On the other hand, the restored signal from the narrower filter has sharp edge; however, the ringing artifacts are produced. After the weighting function is used, the restored signal is obtained with good performance in Fig. 2(h).

IV. Simulation Results

In our simulations, there are two patterns of blurred images. We show two kinds of blurred patterns: the QR code pattern and USAF pattern. They are shown in Figs. 3(a) and 4(a).

Figs. 3(b) and 4(b) are the blurred version of Figs. 3(a) and 4(a), respectively. The blurring effect causes from the PSF and noise. Then, the RL based algorithm [7], the Wiener filter method [9], the pyramid Wiener filter method [10], and our proposed approach are applied to reconstructed the original images and the results are shown in Figs. 3(c)(d)(e)(f) and 4(c)(d)(e)(f), respectively. Then, in Tables I and II, we use mean square error (MSE) and SSIM [8] to measure the quality of the reconstructed image.

From Table I, Table II, Fig. 3, and Fig. 4, it can be seen that the proposed algorithm has better performance than other methods. Moreover, Figs. 3(f) and 4(f) show that our approach is robust to noise in the flat region and has better reconstruction results in the edge region simultaneously. These two goals are hard to achieve at the same time, but can be accomplished by our method.

V. Conclusion

In this paper, we propose an image deblurring algorithm using the edge-membership based reconstruction filter. By using the linear combination of the reconstruction results of short response and long response filters, the original image can be reconstructed efficiently and accurately.

The simulation results show that our approach takes advantage of both images to generate a better restoration images. On the other hand, even on the low spatial resolution image, our approach still has better performance than each other.

Acknowledgment

This work was supported by Industrial Technology Research Institute, Taiwan.

TABLE I
MSE AND SSIM OF THE SIMULATION RESULTS IN FIG. 3.

	MSE	SSIM
Blurred and noisy image of the QR code pattern	0.0603	0.8899
RL based algorithm	0.0214	0.9870
Wiener filter	0.0513	0.9221
Pyramid Wiener filter	0.0744	0.8480
OUR APPROACH	**0.0135**	**0.9950**

TABLE II
MSE AND SSIM OF THE SIMULATION RESULTS IN FIG. 4.

	MSE	SSIM
Blurred and noisy image of USAF	0.1199	0.8728
RL based algorithm	0.0322	0.9919
Wiener filter	0.1384	0.8599
Pyramid Wiener filter	0.1940	0.7112
OUR APPROACH	**0.0278**	**0.9941**

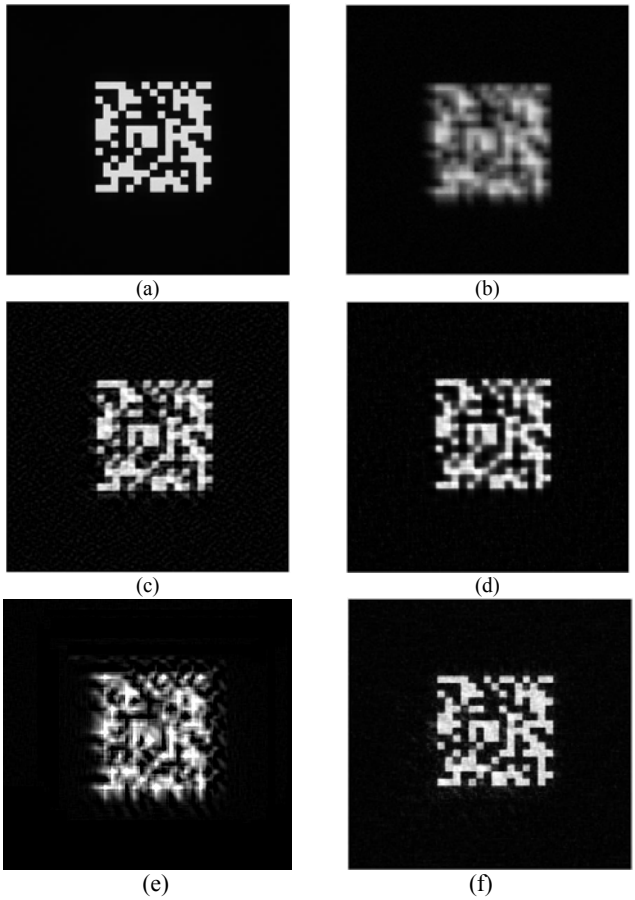

Fig. 3 (a) The original image (the QR code pattern). (b) Blurred image with the interference of the PSF and noise. (c)-(e) The reconstructed images from (c) the RL based algorithm, (d) the Wiener filter, (e) the pyramid Wiener filter, and (f) **our proposed approach**

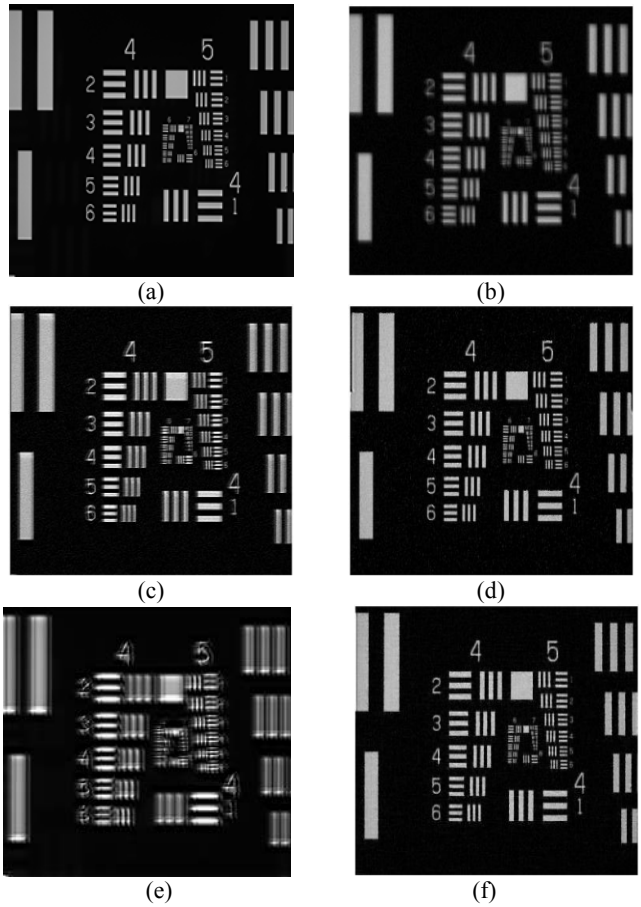

Fig. 4 (a) The original image (the USAF pattern). (b) Blurred image with the interference of the PSF and noise. (c)-(e) The reconstructed images from (c) the RL based algorithm, (d) the Wiener filter, (e) the pyramid Wiener filter, and (f) **our proposed approach**

REFERENCES

[1] M. Asif, A. S. Malik, and T. S. Choi, "3D shape recovery from image defocus using wavelet analysis," *ICIP*, vol. 1, pp. 1025-1028, Sept. 2005

[2] D. Kundur and D. Hatzinakos, "Blind image deconvolution," *IEEE Signal Process. Mag.*, vol. 13, no. 3, pp. 43-64 May 1996.

[3] M. R. Banham and A. K. Katsaggelos, "Digital image restoration," *IEEE Signal Process. Mag.*, vol. 14, pp. 24-41, Mar. 1997.

[4] D. Robinson and D. B. Stork, "Joint design of lens systems and digital image processing," *International Optical Design Conference*, Vancouver, Canada, vol. 6342, June 2006.

[5] R. G. Brown and P. Y. C. Hwang, *Introduction to Random Signals and Applied Kalman Filtering*, Wiley, New York, 1997.

[6] D. Geman, and G. Reynolds, "Constrained restoration and the recovery of discontinuities," *IEEE Trans. Pattern Anal. Mach. Intell.*, vol. 14, no. 3, pp. 367-383, Mar. 1992.

[7] L. Yuan, J. Sun, L. Quan, and H. Y. Shum, "Progressive inter-scale and intra-scale non-blind image deconvolution," *ACM SIGGRAPH*, vol. 27, no. 3, article 74, Aug. 2008.

[8] A. C. Brooks and T. N. Pappas, "Using structural similarity quality metrics to evaluate image compression techniques," *ICASSP*, vol. 1, pp. 873-876, Apr. 2007

[9] P. C. Chen, Y. L. Chen, and H. Y. Sung, "Image restoration based on multiple PSF information with applications to phase-coded image system," *Proc. SPIE*, vol. 7798, pp. 1-9, 2010.

[10] C. Y. Tseng, S. J. Wang, C. W. Chang, P. C. Chen, C. C. Chang, and Y. A. Chen, "Digital image restoration for phase-coded imaging system," *Proc. SPIE*, vol. 7723, pp. 7723-59, 2010.